Dominating migration barrier for intrinsic defects in gallium oxide: dose-rate effect measurements

Alexander Azarov[1,a], Vishnukanthan Venkatachalapathy[1,2], Edouard V. Monakhov[1], and Andrej Yu. Kuznetsov[1,a]

[1)] University of Oslo, Department of Physics, Centre for Materials Science and Nanotechnology, PO Box 1048 Blindern, N-0316 Oslo, Norway

[2)] Department of Materials Science, National Research Nuclear University, "MEPhI", 31 Kashirskoe Hwy, 115409 Moscow, Russian Federation

Ion bombardment provides an opportunity to study basic properties of intrinsic defects in the materials since the accumulation of the radiation induced disorder depends on the balance between defect generation and migration rates. In particular, variation of such parameters as irradiation temperature and ion flux, known in literature as dose-rate effect interconnects the macroscopically measured lattice disorder with the migration barrier of the dominating defects. In this work, we measured the dose-rate effect in monoclinic gallium oxide (β-Ga_2O_3) and extracted its activation energy of 0.8±0.1 eV in the range of 25-250 °C. Accounting that the measurements were performed in the Ga-sublattice and considering 0.8±0.1 eV in the context of theoretical data, we interpreted it as the migration barrier for Ga vacancies in β-Ga_2O_3 limiting the process. Additionally, we observed and took into account an interesting form of the lattice relaxation due to radiation-induced disorder buildup, interpreted in terms of the compressive strain accumulation, potentially trigging phase transitions in Ga_2O_3 lattice.

Keywords: semiconductors, gallium oxide, radiation defects, dose-rate effect

a) Authors to whom correspondence should be addressed: alexander.azarov@smn.uio.no, andrej.kuznetsov@fys.uio.no

Understanding of intrinsic defect energetics and, in particular, their migration barriers is of paramount importance in semiconductors. Indeed, point defects and their complexes affect almost all physical properties of materials and knowing their parameters is critical for defect control needed for the realization of electronic devices. Thus, an effort has been undertaken to deduce these parameters, gradually moving the focus from well-understood semiconductors to new materials attracting attention of the semiconductor community. At present, theoretical predictions of defect migration barriers provide invaluable inputs to guide the research [1]. On the other hand, conclusive experimental measurements of the defect migration barriers are rare. One of the direct methods typically used for studies of defect energetics is based on self-diffusion measurements e.g. as demonstrated for Si [2], SiGe [3], ZnO [4], etc. In its turn, ion bombardment provides possibilities for defect control in the irradiated materials and it can be used for the investigation of intrinsic defect properties [5-10]. Nevertheless, the experimental data are incomplete even for relatively mature semiconductors and, in particular, missing for such new interesting material as gallium oxide (Ga_2O_3); currently arresting attention of the semiconductor research community and mostly known in its thermodynamically stable beta-phase, i.e. as β-Ga_2O_3.

The research interest to β-Ga_2O_3 is promoted by its promising applications for the next generation power electronics, deep UV photodetectors, advanced solar cell passivation, etc. [11,12]. Moreover, as an ultra-wide band gap semiconductor Ga_2O_3 has a potential for use in harsh environments such as space missions, nuclear fusion/fission reactors and high energy physics experiments [13]. In all these applications, deeper understanding of defect generation and their migration properties is crucial for long time reliable operation of electronic devices [13-15]. Finally, it should be mentioned that due to its low symmetry, there are multiple nonequivalent matrix sites in Ga_2O_3 and, consequently, corresponding defects. E.g., there is a plethora of corresponding

vacancies and vacancy complexes in β-Ga_2O_3, attracting attention of both theoreticians [16] and experimentalists [17]. From the theoretical side, Kyrtsos *et al.* [18] have predicted relatively low migration barriers for point defects in β-Ga_2O_3, depending on the charge state and migration path. Specifically, the migration barriers for gallium vacancy (V_{Ga}) and oxygen vacancy (V_O), were reported in the range of 0.5-2.3 and 1.2-4.0 eV, respectively [18]. Meanwhile, in earlier work Blanco *et al.* obtained even lower values, reporting migration barriers of 0.1 and 0.5 eV for V_{Ga} and V_O, respectively [19]. Notably, the migration barriers for self-interstitials were estimated to be even lower in energy [19]. Very recently, V_{Ga} migration barrier of 1.2 eV was experimentally estimated by Ingebrigtsen *et al*. by investigating the electrical conductivity recovery as a function of post irradiation anneals in β-Ga_2O_3 [20]. However, this value measures, in the first place, the thermal stability of already formed secondary defects, potentially including the dissociation energetics too. Thus, in reality the verification of the intrinsic defect migration barriers in β-Ga_2O_3 still remain to be done.

In the present work, we do such experimental estimate of intrinsic defects mobility by measuring so called dose-rate effect in β-Ga_2O_3. Indeed, the dose-rate effect methodology was previously applied to other semiconductors by doing Rutherford backscattering spectrometry channeling (RBS/C) measurements of the lattice disorder. It should be noted that often the dose-rate affect (or ion flux effect) referred to the dependence of the damage formation as a function of the ion flux only, for a fixed implantation temperature [21]. In contrast, in the present paper we use more general approach and measure the dose-rate effect by simultaneously varying the ion irradiation flux and the sample (irradiation) temperature [8,10]. The flux determines the average time interval between neighboring collision impacts, while the temperature controls the defect migration and annihilation – altogether affecting the lattice disorder build-up.

Thus, the activation energy of this process, often referred as the activation energy of the dose-rate effect, is correlated with the migration barrier of the dominating defect under investigation.

By applying the above mentioned methodology to β-Ga_2O_3 in the temperature interval of 25-250 °C, we extracted the activation energy of 0.8 eV and correlated it with migration barrier for V_{Ga}, consistently with the theoretical data [18] and also because the disorder was measured in the Ga-sublattice. Moreover, in the course of the studies, we observed and took into account an interesting form of the lattice relaxation in β-Ga_2O_3 due to radiation-induced disorder buildup interpreted in terms of the compressive strain accumulation, potentially trigging phase transitions in Ga_2O_3 lattice.

Monoclinic (010) β-Ga_2O_3 single crystals, purchased from Tamura Corp., were implanted with 400 keV $^{58}Ni^+$ ions in a wide range of ion fluxes (J = 8×10^{10} - 5×10^{12} at.$cm^{-2}s^{-1}$) and irradiation temperatures (T_i = 25-300 °C) keeping the total accumulated ion dose constant at 6×10^{13} Ni/cm^2. Notably, the irradiation times corresponding to the ion fluxes used in the present work, were in the range of 12-750 s, so even for the highest dose-rate used there were no extra heating of the samples due to ion irradiation. Importantly, the total accumulated dose was small enough to neglect chemical effects of Ni in β-Ga_2O_3 lattice. The implantations were performed in vacuum, maintaining 7° off-normal orientation of the samples to minimize channeling. After implantations the samples were measured by RBS/C using 1.6 MeV He^+ ions incident along [010] direction and backscattered into a detector placed at 165° relative to the incident beam direction. All RBS/C spectra were analyzed using one of the conventional algorithms [22] for extracting the effective number of scattering centers (referred to below as 'relative disorder'). It should be noted that only Ga-parts of the RBS/C spectra were analyzed in details because of the higher sensitivity of the technique as compared to the

O-related signals - due to the mass difference (the Ga signal is higher by the factor of ~15 as compared to that of O for the same concentration). Thus, the activation energy of the dose-rate effect was calculated for Ga-sublattice only. In addition, X-ray diffraction (XRD) 2theta measurements were performed using Bruker AXS D8 Discover diffractometer using Cu $K_{\alpha 1}$ radiation in locked-coupled mode. The strain accumulated due to the defect generation was estimated from the observed shoulder peak positions on the high-angle side of the characteristic (020) β-Ga_2O_3 peak by converting the angular difference into the lattice parameter and corresponding compressive strain. The characteristic XRD peak positions for κ-Ga_2O_3 and ε-Ga_2O_3 were calculated using the VESTA program [23], from the unit cells by Cora *et al.* [24] and Sharma *et al.* [25], respectively.

Fig 1 shows relative disorder accumulation in Ga-sublattice, as measured by RBS/C, as a function of the ion flux and irradiation temperature. The RBS/C spectra in Fig. 1 are characterized by well resolved Gaussian-shape damage peaks located close to the position of the nuclear energy loss profile maximum (R_{pd}=125 nm according to the SRIM code simulations [26] and marked by the arrow in Fig. 1(a)). The amplitudes of the peaks are well below the amorphization level that is equivalent to the height of the random spectrum. The implants at elevated temperatures lead to the dynamic annealing enhancement and significant decrease of the relative disorder already for the 150 and 200 °C implants as compared to room temperature (see Fig. 1(a)). Further increase of the irradiation temperature to 250 °C leads to dramatic reduction of the radiation-induced disorder, as verified by the corresponding RBS/C spectrum moving very close to the virgin one. Importantly, the complimentary role of the ion flux on defect accumulation is illustrated by the RBS/C spectra of the samples implanted at 150 °C with a range of ion fluxes, see Fig. 1(b). It is seen, that the relative disorder decreases

with lowering the ion flux; however, not gradually as will be evident by considering the activation nature of the process.

The process observed in Fig. 1 is a clear manifestation of the dose-rate effect. Fig.2 illustrates the corresponding schematics of the processes, where the effective cascade areas determined by the diffusion of defects, escaped from the thermalized collision cascade core, are shown by tear-shaped regions. Increasing the ion flux at the fixed irradiation temperature increases the probability of appearing neighboring collision cascades (labeled as 2) within a time interval when the defects from the first impact (labeled as 1) are not yet annihilated or stabilized (t_s). That should lead to the overlap of the effective collision cascades and, therefore, increase the number of defects, as illustrated by the left-hand side plot in Fig. 2(a). The average overlapping time of collision cascades (t_{ov}) is an inverse function of ion flux, so that $t_{ov} \sim J^{-1}$. The strength of the dose-rate effect depends on the interrelation between t_{ov} and t_s, so that it is the most pronounced for the condition of $t_{ov} \approx t_s$ (Ref. [27]). In its turn, dynamic annealing becomes more efficient with increasing temperature, so that the defect annihilation/stabilization occurs much faster resulting in the decrease of t_s (right-hand side plot in Fig. 2(a)). Thus, if the ion flux is not high enough, so that $t_{ov} > t_s$, the defects from the first cascade are stabilized or annihilate well before the second impact. Note that for clarity the effective cascade area of the first ion is shown by the reduced tear-shaped region to highlight that this region contains much less mobile defects which can migrate and interact with those from the second impact. Therefore, the disorder accumulation due to cascade overlapping will be not as efficient as for the case of high ion fluxes or low irradiation temperatures. Thus, ion flux and irradiation temperature work together balancing defect generation and annihilation rates where one or another process can dominate depending on J/T_i values.

Taking into account the discussion above, the role of the irradiation temperature and ion flux on the disorder accumulation is schematically illustrated by the panels (b) and (c), respectively. It is seen that, the ion flux range, where the dose-rate effect occurs, shifts towards the higher values with increasing temperature (decrease of t_s). In its turn, higher irradiation temperatures are required to see the dose-rate effect with increasing ion flux (decrease of t_{ov}). In either way, the activation energy of the dose-rate effect will characterize the dominating migration barrier for intrinsic defects.

To unveil this activation energy, the maximum relative disorder, as deduced from the RBS/C results, is plotted as a function of irradiation temperature for three different ion fluxes in Fig. 3. It is clearly seen that the data shift to higher temperatures with increasing ion flux, consistently with the scenario described above and the observations in other semiconductors [4,5]. As it was demonstrated in literature, this trend illustrates the balance between defect generation and annihilation rates, so that the critical transition temperature for each ion flux can be determined according to an averaging methodology described elsewhere [28]. Thus, following this approach critical transition temperatures were determined for each ion flux by fitting the experimental data (symbols in Fig. 3) with an inverse exponential function (lines in Fig. 3). The inset in Fig. 3 shows the Arrhenius plot for the ion flux vs this critical transition temperature determined form the above mentioned procedure. As a result, the Arrhenius analysis gives an activation energy of $E_a = 0.8 \pm 0.1$ eV as a characteristic parameter for the dose-rate effect in β-Ga_2O_3.

As discussed above and visualized by Fig. 2, the dose-rate effect is limited by the diffusion of the defects, so that E_a is related to the corresponding migration barriers. Notable in our experiment, all types of point defects, both in Ga and O sublattices can be generated in the collision cascades. Moreover, the migration barriers of point defects

depend on their charge states that widen the range of potential candidate responsible for the observations in Figs. 1 and 3 even further. However, typically interstitials are highly mobile even at low temperatures, inconsistently with E_a=0.8 eV. In its turn, vacancies are less mobile; more specifically, E_a=0.8 eV is out of the V_O migration barrier range but in accordance with that for V_{Ga} [18]. Additional argument in favor of Ga-related defects to be responsible for E_a=0.8 eV is simply because we analyzed defect evolutions in Ga-sublattice with RBS/C. Thus, we interconnect E_a=0.8 eV from Fig. 3 with the migration barrier for V_{Ga} even though we cannot specify its exact configuration (tetrahedral or octahedral Ga sites). At this end, it is worth to repeat that for the conditions in Fig.1, the disorder buildup is governed by the dynamics of the defect formation during ion irradiation, allowing a direct determination of the defect migration parameters. Meanwhile, the experiments with the post implant anneals, in the first place, test the thermal stability of already formed defects, as it was done e.g. by Ingebrigtsen *et al.* [20].

Fig. 4 summarizes the XRD data of the irradiated samples (selecting the same samples as in Fig. 1 for comparison). Spectacularly, the XRD data are in agreement with RBS/C data. Indeed, the dominating peak at 60.9° in Fig. 4 is the signature of (020) β-Ga_2O_3 diffraction. Using this peak as a reference, there is an interesting trend observed in Fig. 4 upon the implants. Indeed, additional distinct peaks appear on the high-angle side of the (020) β-Ga_2O_3 peak. On the other hand, much less significant changes are observed on the low-angle side of the (020) β-Ga_2O_3 peak.

It should be noted that in majority of cases, the disorder accumulation is associated with the tensile strain buildup, e.g. in ZnO [29], SiC [30] and MoO_3 [31]; moreover, the relaxation via tensile strain in the region implanted with light elements such as Mg and N was observed in β-Ga_2O_3 too [32]. However, our results indicate

negligibly low level of the tensile strain accumulated in the lattice. In contrast, appearing of the high-angle reflections may indicate the compressive strain buildup in the lattice. Assuming the additional peaks on the high-angle side in Fig. 4 characterize the strained lattice, we calculated the magnitudes of this strain and correlated it with the relative disorder accumulation in the RBS/C experiment as illustrated by the inset in Fig. 4(b). Notably, compressive strain buildup was previously observed in ZnO implanted with Yb^+ ions and authors suggested that this effect is attributed to the lattice parameter decrease due to ion-induced oxygen loss from the implanted layer [33]. This mechanism cannot be excluded despite that the oxygen loss should be more pronounced for higher irradiation temperature potentially leading to the higher strain, which is not the case in Fig. 4(a).

In this context, another potential relaxation pathway specifically credible for Ga_2O_3 is associated with its multi-phase nature. Indeed, in addition to thermodynamically stable β-Ga_2O_3, there are several higher energy phases, so that the disorder may enable formation of other phases instead (or in addition) of building up strain in β-Ga_2O_3. Such ion-induced phase transitions were indeed detected by high resolution transmission electron microscopy performed in Ge^+ ion implanted β-Ga_2O_3, revealing the formation of metastable orthorhombic κ-Ga_2O_3 in addition to the defect clusters and extended defects throughout the entire implanted region [34]. A range of possible phases/planes calculated for κ- and ε-Ga_2O_3 are labeled by vertical lines in Fig. 4. Even though, no perfect match is found for the additional reflections in Fig. 4, ion-induced phase transitions cannot be excluded. Notably, the thickness of the ion-beam modified region (~250 nm) is much smaller as compared to the whole XRD probing volume (~12 μm), so that the reflections from the new phases may not be well resolved. Moreover, compressive strain may still potentially occur in β-Ga_2O_3 in response to the

new phase inclusions, consistently with observations of Anber *et al.* [34]. Finally, it should be mentioned that different sign of the ion-induced strain observed in Ref. 32 (implanting Mg and N) and in the present work (Ni) may be attributed to the different orientation of the β-Ga_2O_3 wafers used. Most importantly, the correlation between the RBS/C and XRD data – see the inset in Fig. 4(b) - provides interesting perspectives for further explorations.

In conclusion, by studying radiation accumulation in (010) β-Ga_2O_3 as a function of irradiation temperature and ion flux we observed the dose-rate effect. Accounting that, the ion flux determines the average time interval between neighboring collision impacts, while the temperature controls the defect migration, we interconnected the disorder accumulation with the migration barrier of the dominating defects. More specifically, we correlated the activation energy of the dose-rate effect E_a = 0.8±0.1 eV, with the migration barrier for the Ga vacancies in Ga_2O_3, consistently with the theoretical data. Additionally, we observed and took into account an interesting form of the lattice relaxation due to radiation-induced disorder buildup interpreted in terms of the compressive strain accumulation, potentially trigging phase transitions in Ga_2O_3 lattice.

ACKNOWLEDGMENTS

This work was performed within the Research Centre for Sustainable Solar Cell Technology (FME SuSolTech, project number 257639) and co-sponsored by the Research Council of Norway and industry partners. The Research Council of Norway is acknowledged for the support to the Norwegian Micro- and Nano-Fabrication Facility,

NorFab, project number 295864. The international collaboration was enabled by the INTPART Program at the Research Council of Norway (grant nr 261574).

DATA AVAILABILITY

The data that supports the findings of this study are available within the article.

1. C. Freysoldt, B. Grabowski, T. Hickel, J. Neugebauer, G. Kresse, A. Janotti and C. G. Van de Walle, "First-principles calculations for point defects in solids", Rev. Mod. Phys. **86**, 253 (2014).
2. H. Bracht, H. H. Silvestri, I. D. Sharp, and E. E. Haller, "Self- and foreign-atom diffusion in semiconductor isotope heterostructures. II. Experimental results for silicon", Phys. Rev. B **75**, 035211 (2007).
3. P. Laitinen, A. Strohm, J. Huikari, A. Nieminen, T. Voss, C. Grodon, I. Riihimäki, M. Kummer, J. Äystö, P. Dendooven, J. Räisänen, W. Frank, and the ISOLDE Collaboration, "Self-diffusion of ^{31}Si and ^{71}Ge in relaxed $Si_{0.20}Ge_{0.80}$ layers", Phys. Rev. Lett. **89**, 085902 (2002).
4. A. Azarov, V. Venkatachalapathy, Z. Mei, L. Liu, X. Du, A. Galeckas, E. Monakhov, B.G. Svensson, and A. Kuznetsov, "Self-diffusion measurements in isotopic heterostructures of undoped and *in situ* doped ZnO: Zinc vacancy energetics", Phys. Rev. B **94**, 195208 (2016).
5. H. Bracht, J. F. Pedersen, N. Zangenberg, A. N. Larsen, E. E. Haller, G. Lulli, and M. Posselt, "Radiation enhanced silicon self-diffusion and the silicon vacancy at high temperatures", Phys. Rev. Lett. **91**, 245502 (2003).
6. J. B. Wallace, L. B. Bayu Aji, L. Shao, and S. O. Kucheyev, "Dynamic annealing in Ge studied by pulsed ion beams", Scientific Reports **7**, 13182 (2017).
7. A. Azarov, B. L. Aarseth, L. Vines, A. Hallén, E. Monakhov, and A. Kuznetsov, "Defect annealing kinetics in ZnO implanted with Zn substituting elements: Zn interstitials and Li redistribution", J. Appl. Phys. **125**, 075703 (2019).
8. R. A. Brown and J. S. Williams, "The amorphization kinetics of GaAs irradiated with Si ions", J. Appl. Phys. **83**, 7533 (1998).

9. B. G. Svensson, C. Jagadish, and J. S. Williams, "Generation of point defects in crystalline silicon by MeV heavy ions: dose rate and temperature dependence", Phys. Rev. Lett. **71**, 1860 (1993).

10. A. Yu. Kuznetsov, J. Wong-Leung, A. Hallen, C. Jagadish, and B. G. Svensson, "Dynamic annealing in ion implanted SiC: Flux versus temperature dependence", J. Appl. Phys. **94**, 7112 (2003).

11. S. J. Pearton, J. Yang, P. H. Cary, F. Ren, J. Kim, M. J. Tadjer, and M. A. Mastro, "A review of Ga_2O_3 materials, processing, and devices", Appl. Phys. Rev. **5**, 011301 (2018).

12. "Gallium Oxide Materials Properties, Crystal Growth, and Devices", ed. M. Higashiwaki and S. Fujita, Springer Series in Materials Science **293,** (2020) p. 768.

13. J. Kim, S. J. Pearton, C. Fares, J. Yang, F. Ren, S. Kim, and A. Y. Polyakov, "Radiation damage effects in Ga_2O_3 materials and devices", J. Mater. Chem. C **7**, 10 (2019).

14. Z. Zhang, E. Farzana, W. Y. Sun, J. Chen, E. X. Zhang, D. M. Fleetwood, R. D. Schrimpf, B. McSkimming, E. C. H. Kyle, J. S. Speck, A. R. Arehart, and S. A. Ringel, "Thermal stability of deep level defects induced by high energy proton irradiation in n-type GaN", J. Appl. Phys. **118**, 155701 (2015).

15. G. Yang, S. Jang, F. Ren, S. J. Pearton and J. Kim, "Influence of High-Energy Proton Irradiation on β-Ga_2O_3 Nanobelt Field-Effect Transistors", ACS Appl. Mater. Interfaces 9, 40471 (2017).

16. J. B. Varley, J. R. Weber, A. Janotti, and C. G. Van de Walle, "Oxygen vacancies and donor impurities in β-Ga_2O_3", Appl. Phys. Lett. **97**, 142106 (2010).

17. M. E. Ingebrigtsen, J. B. Varley, A. Yu. Kuznetsov, B. G. Svensson, G. Alfieri, A. Mihaila, U. Badstübner, and L. Vines, "Iron and intrinsic deep level states in Ga_2O_3", Appl. Phys. Lett. **112**, 042104 (2018).

18. A. Kyrtsos, M. Matsubara, and E. Bellotti, "Migration mechanisms and diffusion barriers of vacancies in Ga_2O_3", Phys Rev. B **95**, 245202 (2017).

19. M. A. Blanco, M. B. Sahariah, H. Jiang, A. Costales, and R. Pandey, "Energetics and migration of point defects in Ga_2O_3", Phys. Rev. B **72**, 184103 (2005).

20. M. E. Ingebrigtsen, A. Yu. Kuznetsov, B. G. Svensson, G. Alfieri, A. Mihaila, U. Badst¨ ubner, A. Perron, L. Vines, and J. B. Varley, "Impact of proton irradiation on conductivity and deep level defects in β-Ga_2O_3", APL Mater. **7**, 022510 (2019).

21. S. O. Kucheyev, J. S. Williams, C. Jagadish, J. Zou, and G. Li, "Damage buildup in GaN under ion bombardment", Phys. Rev. B **62**, 7510 (2000).

22. K. Schmid, "Some new aspects for the evaluation of disorder profiles in silicon by backscattering", Radiat. Eff. **17**, 201 (1973).

23. K. Momma and F. Izumi, "VESTA 3 for three-dimensional visualization of crystal, volumetric and morphology data", J. Appl. Crystallogr. **44**, 1272 (2011).

24. I. Cora, F. Mezzadri, F. Boschi, M. Bosi, M. Čaplovičová, G. Calestani, I. Dódony, B. Pécz and R. Fornari, "The real structure of ε-Ga_2O_3 and its relation to κ-phase", Cryst. Eng. Comm. **19**, 1509 (2017).

25. A. Sharma M. Varshney, H. Saraswat, S. Chaudhary, J. Parkash, H.-J. Shin, K.-H. Chae, S.-O. Won, "Nano-structured phases of gallium oxide (GaOOH, α-Ga_2O_3, β-Ga_2O_3, γ-Ga_2O_3, δ-Ga_2O_3, and ε-Ga_2O_3): fabrication, structural, and electronic structure investigations", International Nano Letters **10**, 71 (2020).

26. J. F. Ziegler, M. D. Ziegler, and J. P. Biersack, "SRIM—the stopping and range of ions in matter (2010)", Nucl. Instrum. Methods Phys. Res. B **268,** 1818 **(**2010).

27. A. I. Titov, A. Yu. Azarov, L. M. Nikulina, S. O. Kucheyev, "Mechanism for the molecular effect in Si bombarded with clusters of light atoms", Phys. Rev. B **73**, 064111 (2006).

28. P. J. Schultz, C. Jagadish, M. C. Ridgway, R. G. Elliman, and J. S. Williams, "Crystalline-to-amorphous transition for Si-ion irradiation of Si(100)", Phys. Rev. B **44**, 9118 (1991).

29. A. Turos, P. Jóźwik, M. Wójcik, J. Gaca, R. Ratajczak, and A. Stonert, "Mechanism of damage buildup in ion bombarded ZnO", Acta Materialia **134**, 249 (2017).

30. A. Boulle, A. Debelle, J.B. Wallace, L.B. Bayu Aji, S.O. Kucheyev, "The amorphization of 3C-SiC irradiated at moderately elevated temperatures as revealed by X-ray diffraction", Acta Materialia 140, 250 (2017).

31. D. R. Pereira, C. Díaz-Guerra, M. Peres, S. Magalhães, J. G. Correia, J. G. Marques, A. G. Silva, E. Alves, K. Lorenz, "Engineering strain and conductivity of MoO_3 by ion implantation", Acta Materialia **169**, 15 (2019).

32. M. H. Wong, C.-H. Lin, A. Kuramata, S. Yamakoshi, H. Murakami, Y. Kumagai, and M. Higashiwaki, "Acceptor doping of β-Ga_2O_3 by Mg and N ion implantations", Appl. Phys. Lett. **113**, 102103 (2018).

33. P. P. Michałowski, J. Gaca, M. Wójcik, and A. Turos, "Oxygen out-diffusion and compositional changes in zinc oxide during ytterbium ions bombardment", Nanotechnology **29**, 425710 (2018).

34. E. A. Anber, D. Foley, A. C. Lang, J. Nathaniel, J. L. Hart, M. J. Tadjer, K. D. Hobart, S. Pearton, and M. L. Taheri, "Structural transition and recovery of Ge implanted β-Ga_2O_3", Appl. Phys. Lett. **117**, 152101 (2020).

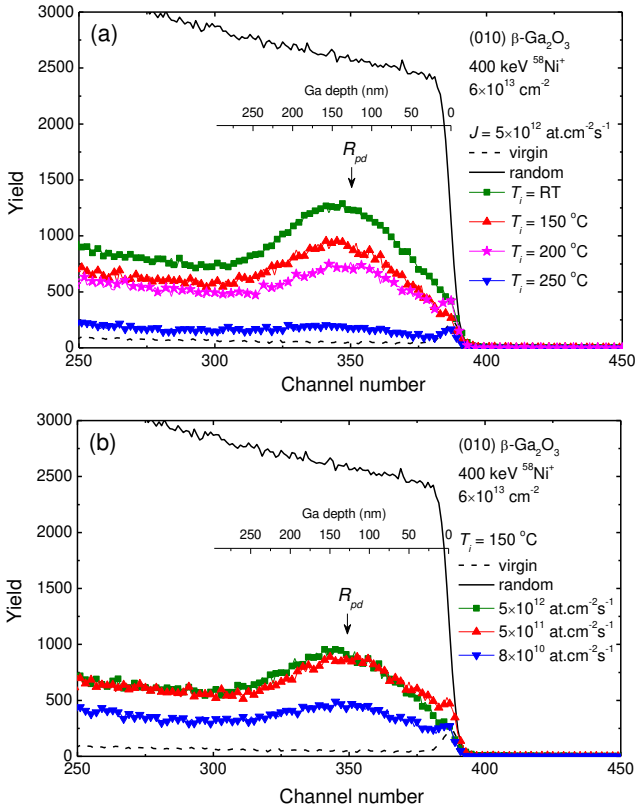

Fig. 1 (a) Relative disorder accumulation in Ga-sublattice as measured by RBS/C in (010) β-Ga_2O_3 implanted with 6×10^{13} Ni/cm^2 at 400 keV; for (a) different irradiation temperatures (T_i) keeping the same ion flux (5×10^{12} at. cm^{-2} s^{-1}) and (b) different ion fluxes (J) keeping the same irradiation temperature (150 °C). The random and virgin (unimplanted) spectra are shown for comparison. The maximum of the nuclear energy loss profile (R_{pd}) predicted with the SRIM code [26] simulations is shown in correlation with the Ga depth scale.

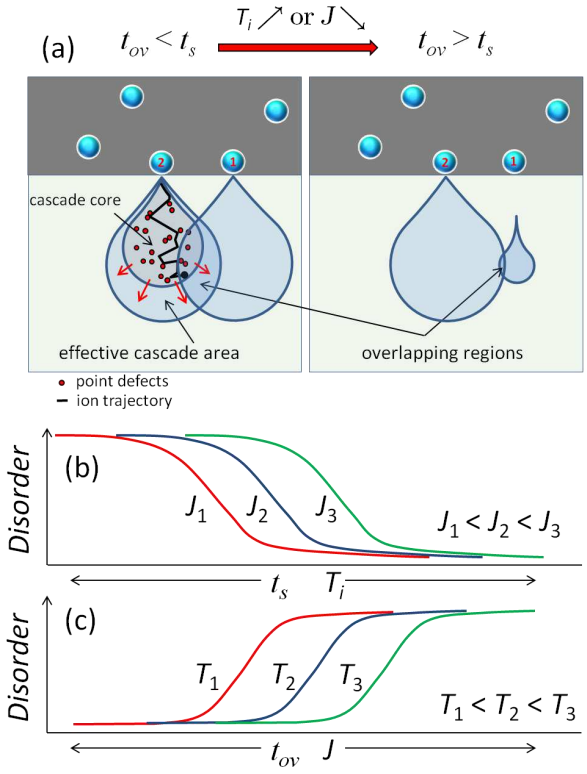

Fig. 2 (a) Schematics of the dose-rate effect balancing the irradiation temperature and ion flux where the ion labeled as 2 hits the surface in the vicinity of the collision cascade created by the first ion (labeled as 1). The characteristic time intervals for collision cascade overlapping (t_{ov}) and defect stabilization (t_s) within effective individual cascades are labeled in the figure. The panels (b) and (c) illustrate of the role of the irradiation temperature for the different ion fluxes and ion flux for the different irradiation temperatures on the disorder accumulation for the constant ion dose.

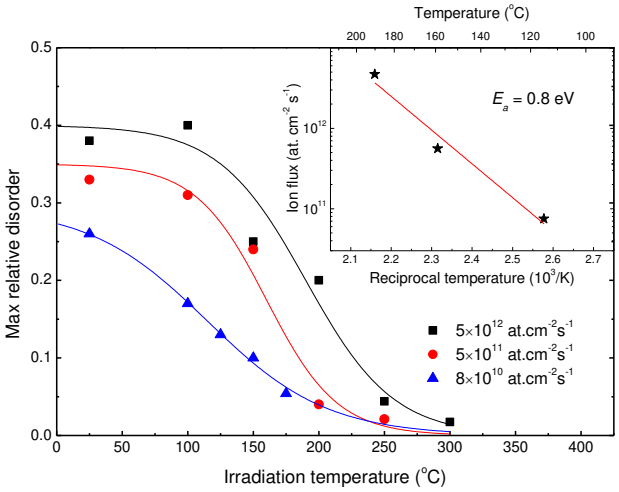

Fig. 3 Maximum relative disorder as deduced from the RBS/C spectra in (010) β-Ga_2O_3 implanted with 400 keV Ni ions to 6×10^{13} cm^{-2} as a function of irradiation temperature for three different ion fluxes as indicated in the legend. The inset shows the Arrhenius plot used to extract the activation energy of the dose-rate effect in β-Ga_2O_3.

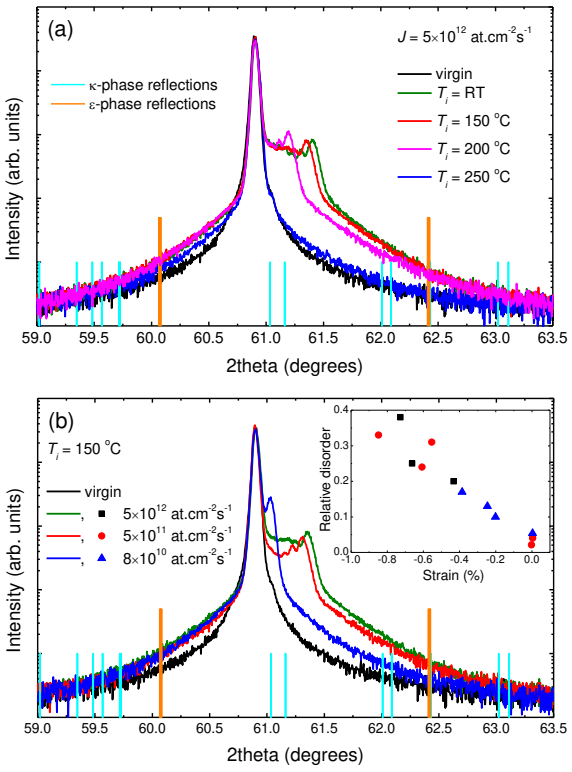

Fig. 4 XRD 2theta scans across (020) reflection of the samples shown in Fig. 1 (a) and (b) illustrating the relaxation in ion implanted β-Ga_2O_3. Vertical lines (light blue and orange) label potential positions for diffraction peaks in κ-Ga_2O_3 and ε-Ga_2O_3, respectively. The inset in panel (b) plots the correlation between the relative disorder and compressive strain attributing the magnitude of the lattice constant change to the minor peaks on the high-angle side of the main peak in Fig 4.